Available online at www.sciencedirect.com

SciVerse ScienceDirect

journal homepage: www.elsevier.com/locate/he

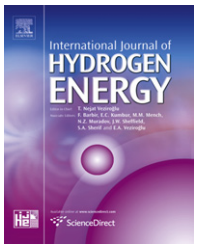

An experimental study of mild flameless combustion of methane/hydrogen mixtures

M. Ayoub [a], C. Rottier [a], S. Carpentier [b], C. Villermaux [b], A.M. Boukhalfa [a], D. Honoré [a,*]

[a] CORIA–CNRS, Université de Rouen et INSA de Rouen, Site Universitaire du Madrillet–BP 8, 76801 Saint Etienne du Rouvray, France
[b] GDF SUEZ, DRI–CRIGEN, 361 avenue du Président Wilson, 93211 Saint Denis La Plaine, France

ARTICLE INFO

Article history:
Received 7 September 2011
Received in revised form
4 January 2012
Accepted 7 January 2012
Available online 31 January 2012

Keywords:
Flameless combustion
Mild combustion
Hydrogen
Furnace
NOx
Chemiluminescence

ABSTRACT

This paper presents an experimental study of mild flameless combustion regime applied to methane/hydrogen mixtures in a laboratory-scale pilot furnace with or without air preheating. Results show that mild flameless combustion regime is achieved from pure methane to pure hydrogen whatever the CH_4/H_2 proportion. The main reaction zone remains lifted from the burner exit, in the mixing layer of fuel and air jets ensuring a large dilution correlated to low NOx emissions whereas CO_2 concentrations obviously decrease with hydrogen proportion. A decrease of NOx emissions is measured for larger quantity of hydrogen due mainly to the decrease of prompt NO formation. Without air preheating, a slight increase of the excess air ratio is required to control CO emissions. For pure hydrogen fuel without air preheating, mild flameless combustion regime leads to operating conditions close to a "zero emission furnace", with ultra-low NOx emissions and without any carbonated species emissions.

1. Introduction

Carbon Capture and Sequestration (CCS) technologies applied to industrial boilers and furnaces have the potential to reduce to about at least 90% of the CO_2 emissions. Pre-combustion technology is one of the technologies considered for the application of CCS to large-scale combustion facilities [1]. In this case, the fuel (gas, liquid or solid) is first reacting in a reformer/gasifier to produce (CO/H_2) syngas, which is after injected in a gas shift reactor where CO reacts with steam to produce (CO_2/H_2) mixture. Then, CO_2 can be captured to be ready for transport and underground storage after cleaning and compression. In an Integrated Gasifier Combined Cycle (IGCC) power plant, resulting hydrogen fuel is used in a gas turbine connected to a steam turbine to produce electricity. CCS pre-combustion technology could be also considered as a kind of centralised generation unit of hydrogen fuel which could be transported and distributed to decentralised applications. This can be expected to be achieved by a gradual transition by adding hydrogen to natural gas. Moreover the decline of fossil fuels availability induces new interest in hydrogen-methane fuel mixtures such as by-products from refineries or industrial plants or biomass-derived fuels. This context shows the interest to study and point out the effect of the use of hydrogen from small to large quantities in combustion applications initially designed to fossil fuel such as natural gas.

Another environmental issue of pollutant emissions from industrial furnaces concerns nitrogen oxides (NOx), because of their multiple impacts on health and environment (lung infection, smog, acid rains, tropospheric ozone production, greenhouse effect, stratospheric ozone depletion,…). Different

* *Corresponding author*. Tel.: +33 232959852; fax: +33 232959780.
E-mail address: david.honore@coria.fr (D. Honoré).

0360-3199/$ – see front matter Copyright © 2012, Hydrogen Energy Publications, LLC. Published by Elsevier Ltd. All rights reserved.
doi:10.1016/j.ijhydene.2012.01.018

ways of formation of NO co-exist in flames, which relative extents depend on flame characteristics [2,3].

The "thermal NO" formation corresponds to the direct oxidation of nitrogen molecules. Predominant in flames at high temperature [3,4] , the thermal route follows the extended Zeldovich mechanism, controlled by the first reaction (1) because of its high activation energy.

$$N_2 + O \rightleftarrows NO + N \quad (1)$$

$$N + O_2 \rightleftarrows NO + O \quad (2)$$

$$N + OH \rightleftarrows NO + H \quad (3)$$

In hydrocarbon flames, another way of nitrogen oxides formation exist which is named "prompt NO" as it appears early in the flame root [5]. It corresponds to the reaction of nitrogen molecules with hydrocarbon fragments – mainly CH – following the Fenimore mechanism:

$$N_2 + CH \rightleftarrows HCN + N \quad (4)$$

Then, hydrogen cyanide molecules HCN react to generate ammonia radicals NHi, which oxidations lead to NO formation [3]. Ten years ago, the spin-forbidden reaction (4) has been reconsidered to a spin-allowed one where N_2 react with CH radicals to form NCN [6]:

$$N_2 + CH \rightleftarrows NCN + H \quad (5)$$

From NCN radicals, NO can be directly generated via reactions with O_2, O and OH. At the same time, reactions of NCN with H and OH induce formation of HCN molecules [7,8] . These cyanide radicals can then react as previously considered in the Fenimore mechanism to form NO via ammonia radicals NHi. Even if the complete kinetic mechanism of prompt NO is not yet elucidated, this route occurs mainly in the hydrocarbon flames roots where CHi radicals are present, and can be favored in rich conditions.

The "N_2O route" of NO formation in flames is initiated by a reaction between nitrogen molecules, oxygen atoms and a third collider M producing N_2O molecules, which then react with O or H atoms to form NO:

$$N_2 + O + M \rightleftarrows N_2O + M \quad (6)$$

$$N_2O + O \rightleftarrows NO + NO \quad (7)$$

$$N_2O + H \rightleftarrows NO + NH \quad (8)$$

Because of the third-body reaction (6), the N_2O route is promoted at high pressure and in lean conditions, and is usually considered negligible in atmospheric flames [2,4,9].

The "NNH route" corresponds to the reaction of nitrogen molecules with H atoms, forming NNH radicals which oxidation by O atoms lead to NO formation [10]:

$$N_2 + H \rightleftarrows NNH \quad (9)$$

$$NNH + O \rightleftarrows NO + NH \quad (10)$$

As the two successive reactions (9) and (10) involve H and O atoms, the NNH route mainly occurs in hydrogenated flames roots. Modelisation of NO formation in a flame via the NNH route is a challenging task as it requires precise estimation of O and H concentrations. This way of NO formation is less pressure and temperature dependent than other routes. The contribution of NNH route to the total NO production in combustion is still in debate, as it is sometimes considered as low or even negligible [11,12] or on the opposite important in hydrogen flames and could be even dominant at low flame temperature such as mild flameless regime [13,14].

Apart from CCS technologies, another way to reduce the CO_2 impact of industrial applications consists in the optimisation of energy efficiency of the combustion process. One of the most effective ways to improve the thermal efficiency is the concept of "Excess Enthalpy Combustion" proposed by Weinberg where large part of enthalpy of hot combustion products is recovered to the combustion system [15]. This concept has been applied in high temperature furnace with recuperative burners equipped with steel heat exchangers allowing large air preheating up to 600 °C–700 °C [16,17]. Better improvement has been obtained with burners equipped with ceramic regenerative systems allowing air preheating up to 1000 °C–1200 °C. Compared to a combustion system without any flue gas heat recovering, this permits the doubling of thermal efficiency and then half of the fuel consumption and CO_2 emissions for a constant heat transfer to the system [17].

Main limitations of the applications of regenerative systems in industrial furnace come from the high temperature achieved in the flame leading to too important levels of NOx emissions with air preheating [18]. At high temperature, NOx emissions from conventional combustion systems come mainly from thermal NO route. The strategies employed to limit NO production is thus to control flame temperature by notably staging of air, fuel or both injections, flue gas reinjection through the burner, or flue gas recirculation in the combustion chamber. Improvements of these concepts for regenerative burners have led to a specific combustion mode in high temperature furnace featuring reduced combustion noise, homogeneous heat transfer in the combustion chamber, no more observable flame structures (but rather some evanescent reactions zones), and above all NOx emissions levels that can be an order of magnitude lower than conventional combustion [19–24].

Because of its colorless feature, this combustion mode has been named flameless combustion or FLOX® (acronym for flameless oxidation) [19,22]. As it has been initially obtained with regenerative burners, it is also named high temperature air combustion (HiTAC) or high preheated air combustion (HPAC) [16,20]. For all regenerative burners operating in flameless regime, the common feature of their designs consists of remote injections of fuel and air, resulting of staging gone to extremes [21]. This characteristic has given also the name FDI (Fuel Direct Injection) and FODI (Fuel/Oxidant Direct Injection) for these operating conditions [23,25]. In this configuration, thanks to high momentum of the jets at the exit of the burner, a very large quantity of hot burnt gases recirculates in the combustion chamber. The recirculation ratio Kv defined as the flow rate of recirculating flue gas over the sum of the flow rates of fuel and air inlets can be typically more than 3 [19].

In a flameless combustion burner, as the reactant injections are far away, the main reaction zones cannot be

attached to the burner. As the burner operates with air excess, some oxygen is still present in recirculating flow with hot combustion products. Then sometimes, a weak reaction zone could be observed around the fuel jets as a diffusion flame between fuel and excess oxygen recirculating with flue gas [16]. But, when they exist, the heat release generated by these diffusion flames remains very low. The main heat release can only begin downstream from the burner exit, in the mixing layer from the location where the reactant jets meet. Along this distance, each of the air and fuel jets mixes with recirculating flue gas by turbulent entrainment process. Combustion occurs then in massive diluted conditions, lowering temperature peaks, temporal and spatial thermal gradients and so NOx emissions. Mild combustion (acronym for moderate or intense low-oxygen dilution) is also another denomination of this combustion regime focused on its dilution feature [26]. Considering a well stirred reactor (i.e. without any aerodynamic consideration), mild combustion regime is achieved when very dilute reactants are preheated to very high temperatures and induce low temperature increase during combustion [26,27].

As the mild flameless combustion regime has been initially obtained with regenerative burners, air preheating was first considered as a prerequisite to reach mild flameless combustion regime, even if its achieving without any initial reactant preheating was already envisaged [19,20]. Nowadays, several experiments have shown that flameless combustion regime can be achieved with modest air preheating [23] and even without any reactant preheating [28–30]. As far as the thermal efficiency is concerned, the flue gas heat recovery is no more performed in the combustion chamber in this case, but could be envisaged elsewhere in the industrial system. However, when mild flameless combustion regime can be achieved without air preheating, NOx emissions are one of the lowest obtained in high temperature furnace.

In summary, a mild flameless combustion burner can be considered as a specific configuration which aerodynamics features induced by the geometry of reactant inlets ensure dilution and heating of the reactants (with or without preheating before injection) by hot recirculating combustion products in order to induce locally mild features in the reaction zone where the main heat release occurs. Following this approach, we retain the term “mild flameless combustion” for this original combustion regime achieved in high temperature furnace.

Several works exist now in literature concerning experimental studies of mild flameless combustion of natural gas, but only few works focus on mild flameless combustion of hydrogen/methane mixture [31–34]. The aim of the present work is to point out the interest of the combination of mild flameless combustion and the use of decarbonated fuel from an experimental study of the effect of hydrogen/methane mixture on main features of mild flameless combustion in terms of flue gas emissions and structures of reaction zones. This work is done in a laboratory-scale facility reproducing mild flameless operating conditions with and without air preheating, and equipped with movable optical accesses to allow the application of laser and imaging diagnostics while maintaining thermal confinement.

2. Experimental setup

2.1. *The laboratory-scale mild flameless combustion facility*

The Fig. 1 presents the laboratory-scale facility named “FOUR” (Furnace with Optical accesses and Upstream Recirculation) [29,35]. It has a rectangular combustion chamber (0.5×0.5 m^2 squared section and 1 m height) insulated by high temperature refractory walls (up to 1500 K). This facility is fully accessible to detailed measurements thanks to removable refractory blocks set at different heights on each sides of the combustion chamber. These blocks ensure high temperature thermal confinement and are equipped with thermocouples for wall temperature measurement. When needed, a block can be replaced by a quartz visualisation window to allow the use of optical diagnostics like chemiluminescence imaging. The exit of the combustion chamber is equipped with a thermocouple and a heated sampling probe to allow flue gas temperature and composition measurements. Oxygen concentration is measured by a paramagnetic analyser (Siemens Oxymat 6) and the concentrations of CH_4, CO, CO_2, NO and NOx (after NO_2 conversion) are measured with non-dispersive infrared analysers (Siemens Ultramat 23).

The Fig. 2 presents the mild flameless burner set on the base of the combustion chamber. It consists of two off-axis fuel injectors (3 mm dia.) spaced 101.4 mm apart, set on either sides of a central air jet (25 mm dia.) ending in a convex divergent shape. In this configuration, recirculation of combustion products inside the furnace is only produced

Fig. 1 – Laboratory-scale facility.

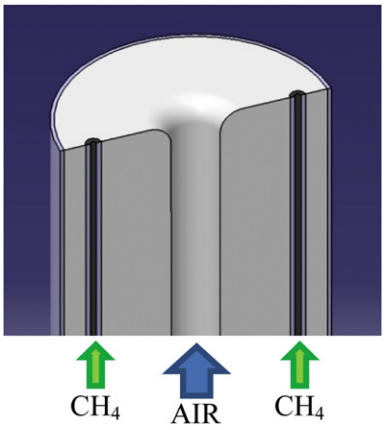

Fig. 2 – The mild flameless burner geometry.

by the jet flows and is controlled by the exit flow characteristics and the geometry of the burner and the combustion chamber. The combustion air can be preheated up to 600 °C thanks to an electric heater, in order to mimic the presence of a regenerative system in the burner but allowing continuous stationary operating conditions. With such burner configuration, combustion cannot be sustained directly when the furnace is at ambient temperature. For that, industrial mild flameless regenerative burners have a "flame mode" where the fuel is injected close to the air jet in order to generate a classical flame attached to the burner during the heating of the furnace. Then, when wall temperature is greater than the self-ignition temperature of the fuel, the burner switches to its "flameless mode": all the fuel is delivered through the distant injectors and mild flameless combustion regime is reached [19,36]. In our case, the heating of the furnace is performed thanks to an external oxy-burner set in a removable block on one side of the combustion chamber. When wall temperature is greater than the fuel self-ignition temperature, this burner is switched off and removed. Mild flameless combustion regime is then achieved with the three jets burner (Fig. 2).

2.2. *Reactive zone visualisation by OH* chemiluminescence imaging*

Some of the chemical reactions occurring during combustion form radicals such as C_2, CH and OH in excited rovibronic levels. As their excited levels are far from the thermodynamic equilibrium, these radicals reach quasi-instantaneously lower rovibronic levels by a spontaneous emission of photons. Then, the collection of such chemiluminescence signal is a convenient way to detect the regions of heat release and obtain the topology of these reaction zones by imaging. Because of the dilution feature of mild flameless combustion regime, chemiluminescence signal from reaction zones is very low compared to a classical flame mode, and largely smaller than the continuous radiation in the visible range coming from hot refractory walls in furnace, inducing its colorless characteristics [36]. However heat release by combustion is still present in the combustion chamber in reaction zones where slight chemiluminescence is emitted. As it occurs in ultraviolet spectral range, OH* chemiluminescence imaging permits to avoid high continuous visible radiation from hot refractory walls in furnace. Then, high sensitivity and dynamic range of intensified CCD (ICCD) cameras allow to record OH* chemiluminescence images even in mild flameless combustion regime in order to obtain and analyse the topology of the reaction zones [37]. In our configuration, OH* chemiluminescence imaging has been implemented on the FOUR facility by using an ICCD camera (Roper Princeton IMAX - 512 × 512 pixel - 16 bits) equipped with a Goyo UV 25 mm f/2.8 lens, and an interferential filter (310 ± 10 nm) to collect OH* chemiluminescence signal through a 100 × 100 mm^2 UV silica window set on one opening of the furnace. To avoid the overheating of the camera, the lens and the filter by wall radiations, a dichroïc UV beam-splitter is used, which transmits the visible and infrared ranges, and reflects perpendicularly a part of the ultraviolet spectral range corresponding to OH* emissions bands. Then the imaging system is set perpendicular to the furnace window and is no more directly exposed to hot radiation. All the optical setup can then be placed as close as possible to the window to optimise the field of view obtained in the combustion chamber (Fig. 3). This configuration ensures the safety of the material, a good spectral selection and a convenient field of view of 200 × 200 mm^2 on the vertical plane centred in the combustion chamber.

2.3. *Experimental methodology*

The operating conditions of the FOUR facility for the present study are summarized in the Table 1. Tests are done with a constant thermal power of 20 kW, with and without air preheating. Two different excess air ratios are tested for non-preheated air cases. For each series of thermal power, excess air ratio and air temperature, the hydrogen volume

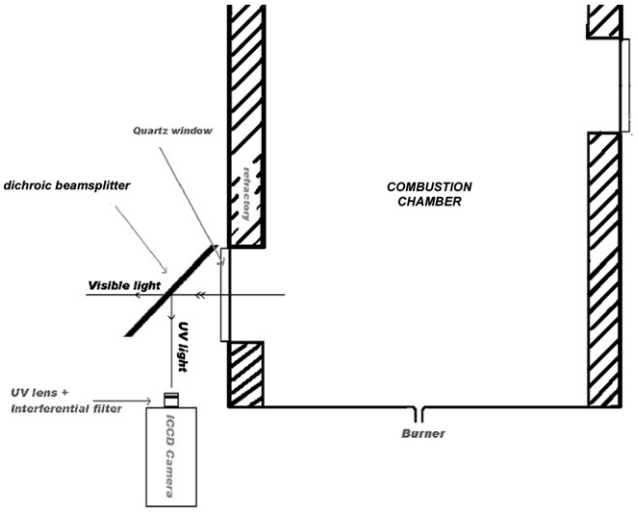

Fig. 3 – The optical setup for safe implementation on the furnace of OH* chemiluminescence imaging with large field of view.

Table 1 – Operating conditions of mild flameless combustion of CH_4–H_2 mixtures.

Test-case	Thermal power P (kW)	Excess air ratio λ (%)	Air inlet temperature Ta (°C)	H_2 proportion (%vol)
T1	20	10	585	0–100
T2	20	11	25	0–100
T3	20	14	25	0–100

proportion in the fuel mixture (CH_4/H_2) is varying from 0 to 100% by step of 10%. Then for each operating conditions, flue gas temperature and composition are measured and reactive zones are recorded by OH* chemiluminescence imaging in regions centred on the exit of the burner and far downstream in the middle part of the combustion chamber. In the following, "MxHy" term represents the operating conditions where the fuel is a mixture of x %vol. of CH_4 and y %vol. of H_2.

3. Main features of mild flameless combustion of CH_4–H_2 fuel with air preheating

Fig. 4 presents the evolution of dry flue gas compositions with the proportion of hydrogen in the fuel, for the operating conditions T1 ($P = 20$ kW – $\lambda = 1.10$ – Ta = 585 °C). Oxygen and carbon dioxide follow theoretical dry compositions of combustion products. No unburnt methane is detected in flue gas. Carbon monoxide concentration increases slightly when adding H_2 in methane but remains always below 10 ppm. From M30H70, it decreases down to a value close to zero.

For small proportions of hydrogen up to M50H50, NO and NOx concentrations show very small variations around constant values of respectively 30 and 40 ppm. From M50H50, they progressively decrease down to 20 and 27 ppm. No increase of NOx emissions is measured unlike other experiments performed with different geometries of mild flameless burners: Donatini et al. observe an increase of NOx emissions from 55 to 88 ppm when adding hydrogen

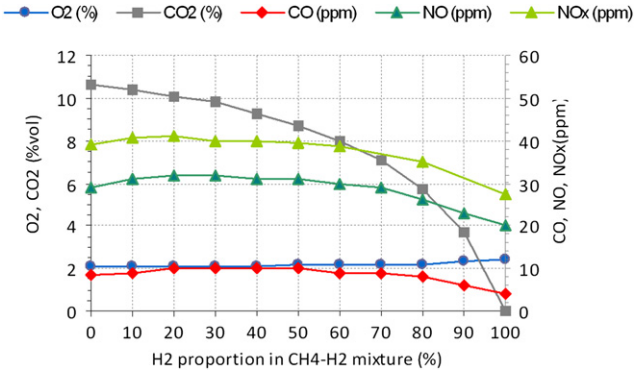

Fig. 4 – Evolution of dry flue gas composition versus H_2 proportion in the fuel (test-case T1: $P = 20$ kW – $\lambda = 1.10$ – Ta = 585 °C).

from 0 to 15% [31]; in a 150 kW facility, Slim et al. measured an increase of NOx emissions from 5 to 42 mg/m^3 associated to the apparition of a visible diffusion flame attached to the burner when H_2 proportion varies from 0 to 75% [32]. In our case, low values of NOx emissions show that mild flameless combustion regime is maintained whatever the CH_4–H_2 proportion.

Mean OH* chemiluminescence images obtained from the average of 500 instantaneous images for the operating conditions T1 are presented Fig. 5. For all CH_4–H_2 proportions, main reactions zones occur from the beginning of both mixing layers between the central air jet and the two fuel jets, and end in the middle part of the combustion chamber. Thanks to their high momentum, turbulent air and fuel jets are diluted by entrainment of recirculating combustion products, before they meet and begin to react [29,38]. As the reaction zones are always lifted, most of the heat release occurs then in hot diluted conditions. This induces very low temperature gradient as well as a moderate maximum value of the temperature [29] and thus explains the very low NOx emissions measured in the present experiment whatever the CH_4–H_2 fuel mixture. Flue gas temperature remains almost constant around 1180 °C, with a maximum gradient of 13 °C (1175 °C for M100H0 to 1188 °C for M0H100). Average wall temperatures vary between 1125 °C for M100H0 and 1155 °C for M0H100.

Significant variation of the lift-off height of the reaction zones is observed when varying CH_4–H_2 composition (Fig. 5). In order to point out the effect of the reaction zones topology on NOx emissions, the height Hb of the beginning of the reaction zones are determined from mean OH* images. For each horizontal line of the image, the pixel locations of the maximum of OH* intensity are determined for both reaction zones on either side of the longitudinal vertical y-axis. Then the longitudinal evolution of OH* maximum intensity is considered, and the lift-off distance Hb is obtained by searching along this profile the height from the burner exit where 5% of the dynamic of OH* maximum intensity is reached. Fig. 6 presents the evolution of Hb with the hydrogen proportion in the fuel with the NO and NOx concentrations. Similar evolution is also observed when considering another threshold value as well as the opposite reaction zone. Except for the pure hydrogen case, one can see a specific relationship between Hb and the resulting NOx emissions.

When the H_2 proportion in fuel varies from 0 to 20%, reaction zones are stabilized closer to the burner. This can be attributed to the high reactivity of hydrogen compared to methane. Indeed, progressive addition of hydrogen in methane induces an exponential increase of laminar burning velocity [39,40] and a more robust sensitivity of turbulent flames to stretch rate [41]. Addition of hydrogen to methane has already proven to be a convenient way to enhance combustion features, in standard non-diluted conditions, for example when adding up to 20% of H_2 in a swirl burner [42], as well as in mild flameless conditions, where the combustion stability and limits of dilution are widened [34], and heat release can be intensified [43]. In our case, as Hb decreases, the entrainment ratio of inert hot combustion products by reactant jets achieved at the locations where reactions begin is

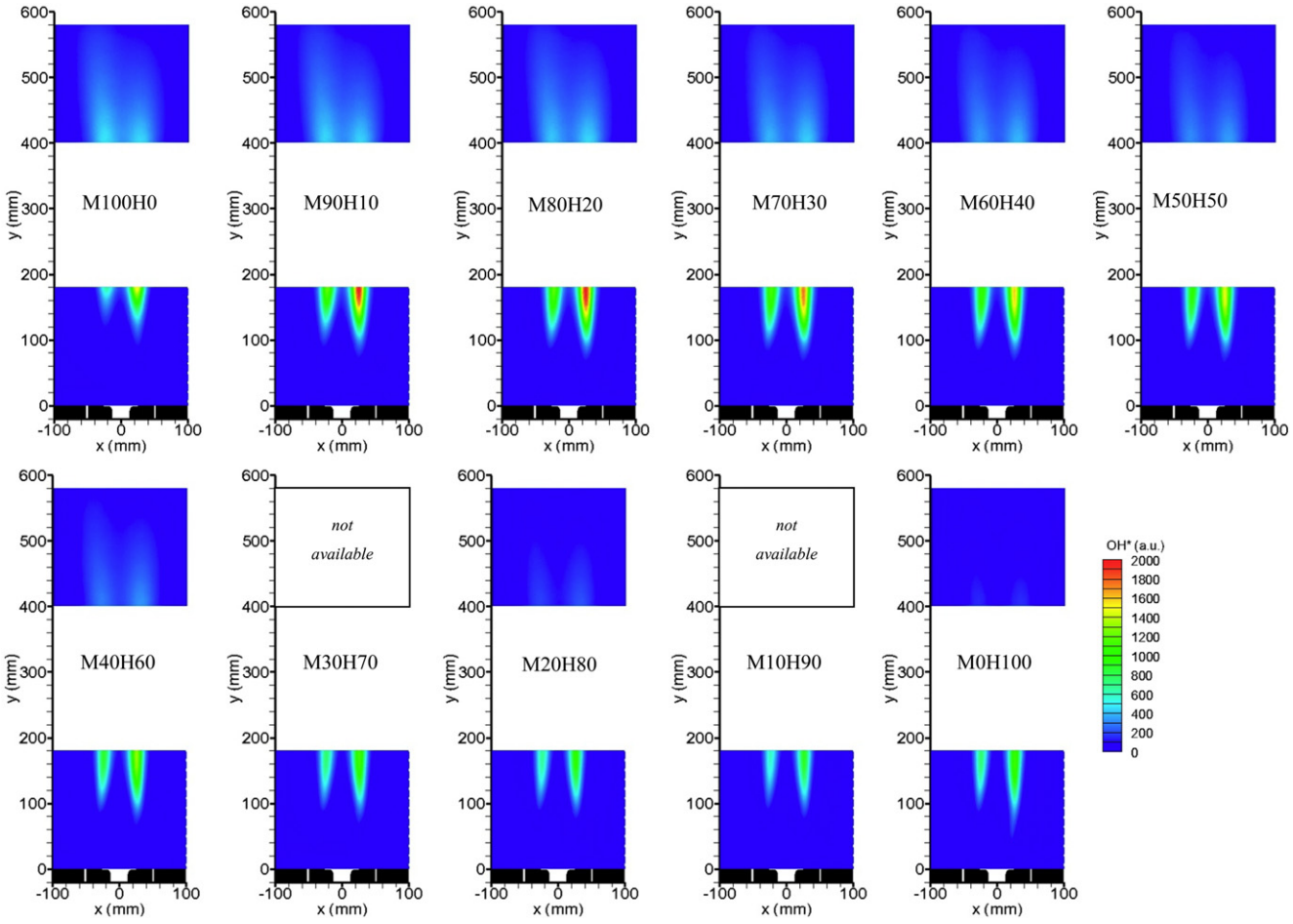

Fig. 5 – Mean OH* chemiluminescence images versus H_2 proportion in the fuel (test-case T1: P = 20 kW – λ = 1.10 – Ta = 585 °C).

smaller. Then combustion occurs in less diluted environment. We can expect a higher local heat release as the OH* chemiluminescence intensity in the reaction zone is also increasing (Fig. 5).

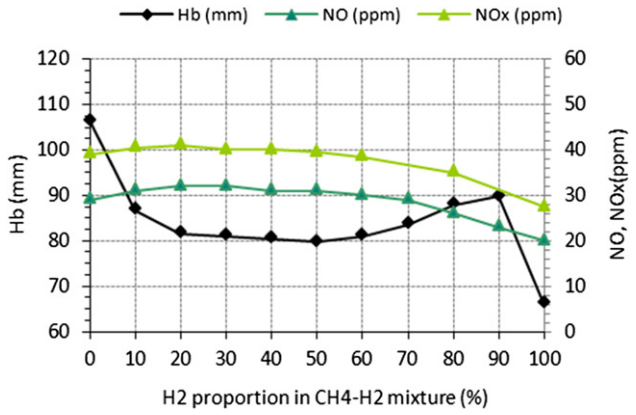

Fig. 6 – Evolutions of the lift-off height Hb of the reaction zone with NO and NOx concentrations versus H_2 proportion in the fuel (test-case T1: P = 20 kW – λ = 1.10 – Ta = 585 °C).

For the NOx emission mechanism, as the overall formation rate of thermal NO strongly depends on local temperature [2], in a more pronounced way than the NNH route [9], the slight increase measured for NOx emissions could be attributed to a slight increase of thermal NO formation as the combustion is less diluted. From M80H20 to M50H50, Hb seems to reach a minimum value (Hb ≈ 80 mm), which corresponds to the beginning of the jets interaction, whereas NOx emissions keep quasi-constant levels. Evolution of Hb is reversed from M50H50. As it is more and more lifted, the reaction zone is more diluted and less intense. One can expect a lower NO formation from thermal route. A very specific behaviour is observed for the pure hydrogen case. Besides the main reaction zone starting from the beginning of the mixing layers between air and fuel jets, a thin reaction zone occurs early around the air jet because of the high diffusivity of hydrogen, as shown on OH* chemiluminescence image even if it is still not visible. Because of its low intensity, this reaction zone has no effect on NOx emissions which are rather controlled by another phenomenon related to large proportion of hydrogen in the fuel.

The decrease of NOx concentrations for large H_2 proportion shows that the NNH route would not provide

a major contribution to NOx emissions. As reflected from CO and CO_2 concentrations evolutions (Fig. 4), decrease of C/H ratio in fuel mixture is more pronounced for large H_2 proportion. As the NO formation via the prompt route corresponds to the reactions of nitrogen with hydrocarbon radicals, a similar decrease can be expected to the C/H ratio and the prompt NO formation, down to its cancellation for pure hydrogen case. This has been already observed by Rortveit et al. when adding hydrogen to methane in porous media inert burners [9]. In the same manner, in our case for mild flameless combustion, the decrease of NO and NOx concentrations for large hydrogen proportion can be attributed to the key effect of the cancellation of prompt NO formation, even if the reaction zone moves upstream for pure hydrogen case.

4. Main features of mild flameless combustion of CH_4–H_2 fuel without air preheating

Previous experiments with pure methane have shown the important effect of air temperature on the structure of reaction zones and its consequence on NOx emissions [29,30]. Fig. 7 presents the evolution of dry flue gas concentrations with CH_4–H_2 composition for the test-case T2 ($P = 20$ kW $- \lambda = 1.11 -$ Ta $= 25$ °C). NOx concentrations are very low – never exceeding 16 ppm - whatever the H_2 proportion in the fuel. However one can observe that the progressive addition of hydrogen in the fuel induces a quick growth of CO emissions reaching values around 50 ppm, before it naturally cancels from M20H80 because of the decrease of C/H ratio. Similar increase of CO concentrations has been observed by Derudi et al. for high recirculation ratio where the oxygen concentration is too small to allow complete oxidation [34]. Such high values of CO concentrations prohibit these operating conditions despite the combustion stability and low NOx emissions.

To avoid CO emissions, the air flow rate has been increased to ensure oxidation of CO in the combustion chamber. This leads to new operating conditions without air preheating for a constant thermal power of 20 kW and a new excess air ratio of 1.14 (Test-case T3 in Table 1). Evolutions of

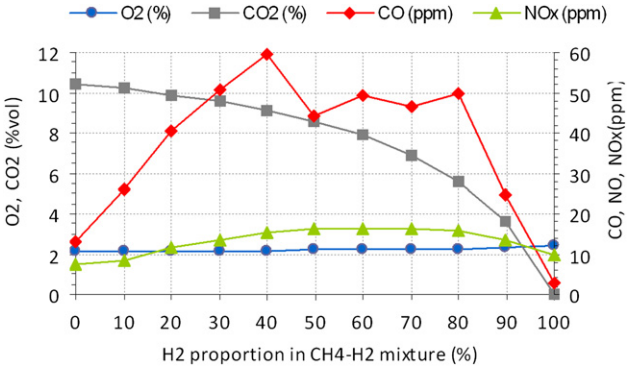

Fig. 7 – Evolution of dry flue gas composition versus H_2 proportion in the fuel (test-case T2: $P = 20$ kW $- \lambda = 1.11 -$ Ta $= 25$ °C).

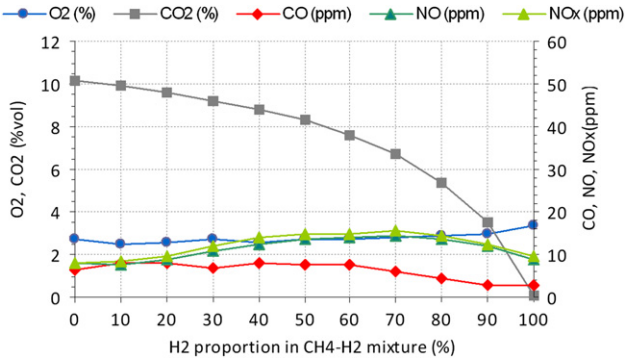

Fig. 8 – Evolution of dry flue gas composition versus H_2 proportion in the fuel (test-case T3: $P = 20$ kW $- \lambda = 1.14 -$ Ta $= 25$ °C).

dry flue gas compositions for these operating conditions are presented on Fig. 8. Oxygen and carbon dioxide variations correspond to theoretical compositions of combustion products. Thanks to the increase of excess air ratio, CO emissions are now controlled and remain lower than 8 ppm for all CH_4–H_2 compositions. As already observed for the test-case T1 with air preheating, CO concentrations gradually decrease from M40H60 following CO_2 concentrations, down to a quasi-zero value. For mild flameless combustion regime, an increase of excess air ratio could induce an important increase of NOx emissions [44]. In the present case, the excess air ratio required to limit CO emissions remains small enough to keep ultra-low NOx emissions whatever the CH_4–H_2 composition. Even if they never exceed 16 ppm, one could observe nevertheless an increase of NOx emissions with the hydrogen proportion in the fuel, more significant than the previous case with air preheating and this time in concordance with other experiments [31,32]. In our case, studying mild flameless combustion in the complete range of CH_4–H_2 mixtures, a decrease of NO and NOx concentration is measured for high proportion of H_2, as previously with air preheating. Without air preheating, NOx concentrations decreases from 16 ppm for M30H70 down to values less than 10 ppm for pure hydrogen operating conditions as for the pure methane ones.

As previously observed for the preheated air case, the decrease of NOx for large proportion of hydrogen indicates that the NNH route would not have a significant role for NO formation in our case. Here, the evolution of NOx with the proportion of H_2 in the fuel can be rather considered to be controlled by two opposite phenomena: one relating to the cancellation of prompt NO when decreasing C/H ratio of the fuel mixture, the other relating to the increase of thermal NO formation associated to the upstream shift of the lifted reaction zone. Without air preheating, mild flameless combustion of pure methane is stabilized far downstream from the burner, ensuring their massive dilution. The smooth gradient and low maximum temperature in the reaction zones induce minimization of NO formation by thermal route and then the ultra-low NOx emissions measured in this case [29]. As shown on mean OH*

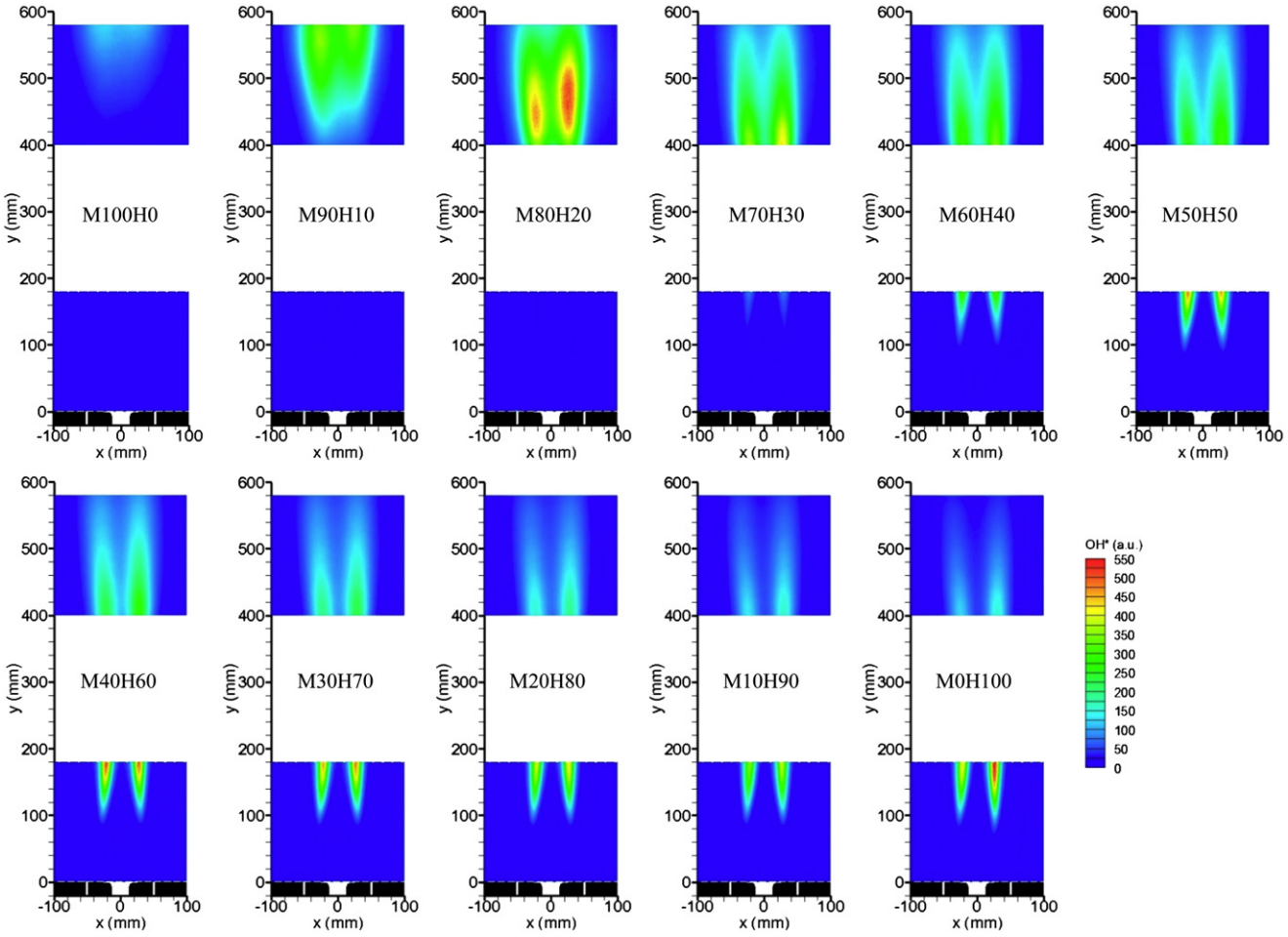

Fig. 9 – Mean OH* chemiluminescence images versus H_2 proportion in the fuel (test-case T3: P = 20 kW – λ = 1.14 – Ta = 25 °C).

chemiluminescence images presented Fig. 9, the progressive addition of hydrogen in the fuel mixture has a tremendous effect on the localization of reactions zones in the furnace. Similar features have been also observed for the test-case T2 despite the high CO emissions (Fig. 11). The evolution of the lift-off height Hb with the H_2 proportion is presented on Fig. 10 for the test-case T3. The doubling of NO and NOx concentrations from M100H0 to M30H70 corresponds to the wide upstream displacement of the reaction zone along the stoichiometric line in the mixing layers between air and fuel jets, from the second half of the combustion chamber to the location of the reactant jets meeting. This induces a decrease of the dilution ratio in the reaction zone. Increase of NOx emissions measured from M100H0 to M30H70 can then be directly attributed to the increase of thermal NO formation due to a larger local heat release density in the less diluted reaction zone. Similar correlation between reaction zone locations and NOx emissions can be pointed out on the results of CFD simulation of mild flameless combustion for different CH_4–H_2 compositions performed by Parente et al. [45]. In the present work, whereas the height of the lifted reaction zone continues to decrease slightly, the decrease of NOx emissions from M30H70 to M0H100 comes thus directly from the cancellation of the prompt NO formation ensuing the cancellation of C/H ratio of the fuel mixture. For pure hydrogen without air preheating, one achieves stable mild flameless combustion close to "zero emission" features

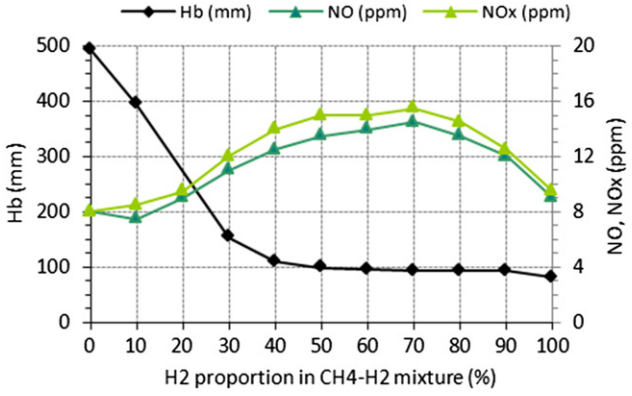

Fig. 10 – Evolutions of the lift-off height Hb of the reaction zone with NO and NOx concentrations versus H_2 proportion in the fuel (test-case T3: P = 20 kW – λ = 1.14 – Ta = 25 °C).

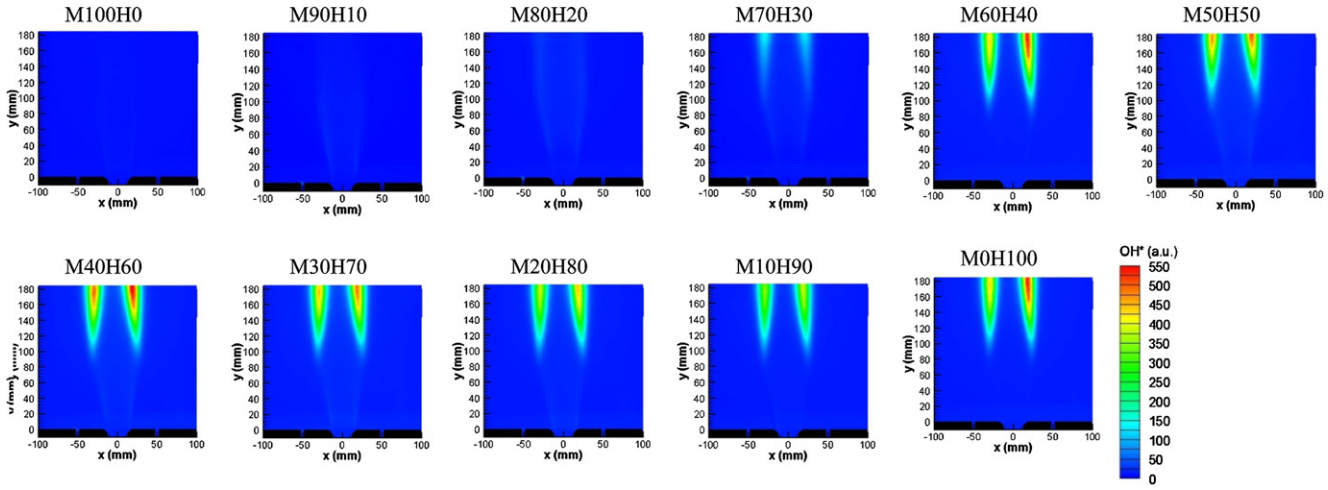

Fig. 11 – Mean OH* chemiluminescence images versus H_2 proportion in the fuel (test-case T2: P = 20 kW – λ = 1.11 – Ta = 25 °C).

without any CO_2 emissions and pollutant concentrations below 10 ppm.

5. Conclusions

The effect of the composition of methane/hydrogen mixture on mild flameless combustion is studied on a laboratory-scale facility. Flue gas composition measurements and reaction zone topology by OH* chemiluminescence imaging are performed for different CH_4/H_2 proportions at constant combustion thermal power with and without air preheating. Mild flameless combustion regime is always achieved whatever the composition from pure methane to pure hydrogen.

Different features are observed for CO emissions when air is preheated or not. With air preheating and an excess air ratio of 10%, CO concentrations always remain below 10 ppm. Without air preheating, an increase of excess air ratio to 14% is required to control CO concentrations without nevertheless an increase of NOx emissions.

The evolution of NOx emissions when varying the hydrogen proportion in the fuel mixture can be divided in two parts. For low hydrogen proportion, NOx concentrations are correlated to the structure of the reaction zone revealed from OH* chemiluminescence imaging. Small addition of hydrogen in methane fuel induces a shifting of the beginning of the reaction zone upstream in the furnace because of the high diffusivity and reactivity of H_2. The reaction zone is so less diluted by entrainment of turbulent jets. Then, a larger local heat release is expected, which explains the increase of NOx emissions measured in flue gas because of larger thermal NO formation. This effect is more noteworthy without air preheating as the upstream shift of the beginning of the reaction zone is large when progressively adding hydrogen in methane. Another evolution is observed from 70% of hydrogen in the fuel mixture: a decrease of NOx concentrations is measured which is no more correlated to the location of the reaction zone, but is rather function of the carbon species concentrations in the fuel. This corresponds to the progressive decrease of NO formation from the prompt route, down to its complete cancellation for pure hydrogen.

In the context of the progressive use of hydrogen on the road to alternative decarbonated fuels, mild flameless combustion proves to be one of the most promising solutions to combine energy efficiency, low pollutant and CO_2 emissions. For pure hydrogen fuel without air preheating, mild flameless combustion regime leads to operating conditions close to a "zero emission furnace", with ultra-low NOx emissions (below 10 ppm) and without any HC, CO and CO_2 emissions.

Acknowledgments

This work is done with the financial support of ADEME (French Agency for Environment and Energy Management) and ANR (PAN-H program).

REFERENCES

[1] Cormos CC. Evaluation of power generation schemes based on hydrogen-fuelled combined cycle with carbon capture and storage (CCS). Int J Hydrogen Energy 2011;36:3726–38.
[2] Bowman CT. Kinetics of pollutant formation and destruction in combustion. Prog Energy Combust Sci 1975;1:33–45.
[3] Beer JM. Minimizing NOx emissions from stationary combustion; reaction engineering methodology. Chem Eng Sci 1994;49(24A):4067–83.
[4] Skottene M, Rian KE. A study of NOx formation in hydrogen flames. Int J Hydrogen Energy 2007;32:3572–85.
[5] De Soete GG. Overall reaction rates of NO and N_2 formation from fuel nitrogen. Proc Combust Inst 1975;15:1093–102.
[6] Moskaleva LV, Lin MC. Computational study of the kinetics and mechanisms for the reaction of H atoms with C-C_5H_6. Proc Combust Inst 2002;29(1):1319–27.
[7] Lamoureux N, Desgroux P, El Bakali A, Pauwels JF. Experimental and numerical study of the role of NCN in

prompt-NO formation in low-pressure CH_4-O_2-N_2 and C_2H_2-O_2-N_2 flames. Combust Flame 2010;157(10):1929–41.
[8] Konnov AA. Implementation of the NCN pathway of prompt-NO formation in the detailed reaction mechanism. Combust Flame 2009;156(11):2093–105.
[9] Rortveit GJ, Zepter K, Skreiberg O, Fossum M, Hustad JE. A comparison of low-NOx burners for combustion of methane and hydrogen mixtures. Proc Combust Inst 2002;29:1123–9.
[10] Bozzelli JW, Dean AM. O + NNH: a possible new route for NOx formation in flames. Int J Chem Kinet 1995;27:1097–109.
[11] Harrington JE, Smith GP, Berg PA, Noble AR, Jeffries JB, Crosley DR. Evidence for a new NO production mechanism in flames. Proc Combust Inst 1996;26(2):2133–8.
[12] Haworth NL, Mackie JC, Bacskay GB. An ab initio quatum chemical and kinetic study of the NNH + O reaction potential energy surface: how important is this route to NO in combustion? J Phys Chem A 2003;107:6792–803.
[13] Konnov AA. On the relative importance of different routes forming NO in hydrogen flames. Combust Flame 2003;134(4): 421–4.
[14] Galletti C, Parente A, Derudi M, Rota R, Tognotti L. Numerical and experimental analysis of NO emissions from a lab-scale burner fed with hydrogen-enriched fuels and operating in MILD combustion. Int J Hydrogen Energy 2009;34:8339–51.
[15] Weinberg FJ. Combustion temperatures: the future? Nature 1971;233:239–41.
[16] Tsuji H, Gupta AK, Hasegawa T, Katsuki M, Kishimoto K, Morita M. High temperature air combustion. From energy conservation to pollution reduction. Boca Raton: CRC Press LLC; 2003.
[17] Flamme M, Boss M, Brune M, Lynen A, Heym J, Wünning JA, et al. Improvement of energy saving with new ceramic self-recuperative burners. Proceedings of the International Gas Research Conference; 1998. San Diego, USA.
[18] Fujimori T, Hamano Y, Sato J. Radiative heat loss and NOx emission of turbulent jet flames in preheated air up to 1230 K. Proc Combust Inst 2000;28:455–61.
[19] Wünning JA, Wünning JG. Flameless oxidation to reduce thermal NO-formation. Prog Energy Combust Sci 1997;23:81–4.
[20] Katsuki M, Hasegawa T. The science and technology of combustion in highly preheated air. Proc Combust Inst 1998; 27:3135–46.
[21] Weber R, Verlaan AL, Orsino S, Lallemant N. On emerging furnace design methodology that provides substantial energy savings and drastic reductions in CO_2 and NOx emissions. J Inst Energy 1999;72:77–83.
[22] Milani A, Saponaro A. Diluted combustion technologies. IFRF Combust J; 2001:200101.
[23] Sobiesiak A, Rahbar S, Becker HA. Performance characteristics of the novel low-NOx CGRI burner for use with high air preheat. Combust Flame 1998;115:93–125.
[24] Flamme M. Low NOx combustion technologies for high temperature applications. Energy Convers Manag 2001;42: 1919–35.
[25] Fleck BA, Sobiesiak A, Becker HA. Experimental and numerical investigation of the novel low NOx CGRI burner. Combust Sci Technol 2000;161:89–112.
[26] Cavaliere A, De Joannon M. Mild combustion. Prog Energy Combust Sci 2004;30:329–66.
[27] De Joannon M, Cavaliere A, Faravelli R, Ranzi E, Sabia P, Tregrossi A. Analysis of process parameters for steady operations in methane mild combustion technology. Proc Combust Inst 2005;30:2605–12.
[28] Masson E. Etude expérimentale des champs dynamiques et scalaires de la combustion sans flamme. Doctoral thesis INSA de Rouen 2005.
[29] Rottier C, Lacour C, Godard G, Taupin B, Porcheron L, Hauguel R, et al. On the effect of air temperature on mild flameless combustion regime of high temperature furnace. Proceedings of the 4th European Combustion Meeting; 2009 April 14–17. Vienna, Austria.
[30] Szegö GG, Dally BB, Nathan GJ. Operational characteristics of a parallel jet MILD combustion burner system. Combust Flame 2009;156:429–38.
[31] Donatini F, Schiavetti M, Gigliucci G, Gheri P, Monticelli M, Mangione R, et al. CFD simulation and experimental tests on a natural gas/hydrogen mixture-fired flameless combustor. Proceedings of the ECCOMAS Thematic Conference on Computational Combustion; 2005 June 21–24. Lisbon, Portugal.
[32] Slim BK, Darmeveil H, Van Dijk GHJ, Last D, Pieters GT, Rotink MH, et al. Should we add hydrogen to the natural gas grid to reduce CO_2 emissions? (consequences for gas utilization equipment). Proceedings of the 23rd World Gas Conference; 2006. Amsterdam, The Netherlands.
[33] Derudi M, Villani A, Rota R. Sustainability of mild combustion of hydrogen-containing hybrid fuels. Proc Combust Inst 2007;31:3393–400.
[34] Derudi M, Villani A, Rota R. Mild combustion of industrial hydrogen-containing byproducts. Ind Eng Chem Res 2007;46: 6806–11.
[35] Rottier C, Lacour C, Godard G, Taupin B, Boukhalfa AM, Honoré D, et al. Velocity and temperature measurements in a laboratory-scale furnace operating in flameless (mild) combustion regime. Proceedings of the 15th IFRF Member's Conference; 2007 June 13-15 [Pisa, Italy].
[36] Plessing T, Peters N, Wünning JG. Laseroptical investigation of highly preheated combustion with strong exhaust gas recirculation. Proc Combust Inst 1998;27:3197–204.
[37] Honoré D. Advanced measurements in industrial combustion systems. In: Vervisch L, Veynante D, Van Beeck JPAJ, editors. Turbulent combustion. Rhode Saint Genèse: von Karman Institute for Fluid Dynamics; 2007.
[38] Mancini M, Schwöppe P, Weber R, Orsino S. On mathematical modelling of flameless combustion. Combust Flame 2007;150:54–7.
[39] Ilbas M, Crayford AP, Yılmaz I, Bowen PJ, Syred N. Laminar-burning velocities of hydrogen–air and hydrogen–methane–air mixtures: an experimental study. Int J Hydrogen Energy 2006;31:1768–79.
[40] Huang Z, Zhang Y, Zeng K, Liu B, Wang Q, Jiang D. Measurements of laminar burning velocities for natural gas-hydrogen-air mixture. Combust Flame 2006;146: 302–11.
[41] Fairweather M, Ormsby MP, Sheppard CGW, Wooley R. Turbulent burning rates of methane and methane-hydrogen mixtures. Combust Flame 2009;156:780–90.
[42] Schefer RW. Hydrogen enrichment for improved lean flame stability. Int J Hydrogen Energy 2003;28:1131–41.
[43] Mardani A, Tabejamaat S. Effect of hydrogen on hydrogen-methane turbulent non-premixed flame under MILD condition. Int J Hydrogen Energy 2010;35: 11324–31.
[44] Masson E, Maurel S, Porcheron L, Aguilé F, Meunier P, Quinqueneau A, et al. An experimental characterization of flameless combustion at semi-industrial scale. Proceedings of the 14th IFRF Member's Conference; 2004 May 11–14. Noordwijkerhoot, The Netherlands.
[45] Parente A, Galletti C, Tognotti L. Effect of the combustion model and kinetic mechanism on the MILD combustion in an industrial burner fed with hydrogen enriched fuels. Int J Hydrogen Energy 2008;33:7553–64.